

# Visual Analysis of Air Traffic Data

## Abstract

*Air travel plays a crucial role in the functioning of today's globalized world. There are over 300,000 flights within the United States every day. In the future, daily air traffic number of all varieties are expected to continue rising. In addition, there is increasing interest in integrating unmanned aerial vehicles, for both government and commercial interests, into the national airspace system (NAS). This large growth in aviation operations will only increase traffic within the already limited NAS, leading to higher congestion and less free airspace. In this paper, we present visual analysis tools to study the impact of policy changes on air traffic congestion. The tools support visualization of time-varying air traffic density over an area of interest using different time granularity. We use this visual analysis platform to investigate how changing the aircraft separation volume can reduce congestion while maintaining key safety requirements. The same tool can also be used as a decision aid for processing requests for unmanned aerial vehicle operations.*

## 1. Introduction

Aviation and air travel has established itself as a key economic and social resource in modern times. As the world population increases and becomes ever more interconnected, the demand for air travel will only increase. Currently there are over 100,000 commercial aviation flights and over 200,000 general aviation flights within the national airspace system (NAS) every day. This does not include military sorties or other, special purpose, flights within the NAS. The number of passengers flying to or from the U.S. is expected to grow an average of 4.5% annually, with cargo amounts showing a similar increase, while general aviation is expected to grow 1% annually. In addition, there is increasing interest, from both government and commercial sectors, in integrating unmanned aerial vehicles (UAV's) into the NAS. Though full UAV integration poses its own unique set of complications, nevertheless it is only a

matter of time before they contribute to the air traffic over the NAS. This constant increase in air traffic within the increasingly congested NAS will require new methods and techniques to efficiently accommodate new traffic.

To address these issues, the US Congress approved plans for the development of the Next Generation Air Transportation System (NextGen). It is an overhaul of the current NAS with the goals of allowing more aircraft to safely fly closer together with more direct routes. It is scheduled for implementation in stages between 2012 and 2025 with 5 major elements: (i) Automatic dependent surveillance-broadcast (ADS-B) will replace radar systems with satellite based global positioning information for each aircraft. This information will be broadcast in realtime to airports and other aircraft within a 150 mile radius allowing them to fly closer without jeopardizing safety. (ii) System wide information management (SWIM) is a consolidation of multiple information systems into a single coherent system and will reduce redundancy and facilitate information sharing. (iii) NextGen data communication will add data links between aircraft and air traffic controllers to the current two-way voice communication. (iv) NextGen network enabled weather is an ambitious effort to fuse data from tens of thousands of ground, air, and space based sensors into a single national weather information system to provide realtime weather information. (v) NAS voice switch (NVS) will replace multiple existing voice switching systems into a single consolidated air/ground and ground/ground voice communication system.

The NextGen system will provide the infrastructure to allow aircraft to safely fly closer together thereby making more efficient use of limited airspace. It will allow aircraft to use more direct routes instead of being constrained to predetermined sky highways thereby reducing congestion and reduce fuel costs.

With pieces of the NextGen infrastructure coming into place, there is an opportunity to further their benefits by developing software tools that provide added value. This paper focuses on such a software – a visual analysis tool that allows policy makers to see the effects

of changing the aircraft separation volume on congestion. The same tool can also be used as a decision aid for processing requests for unmanned aerial vehicle operations. Specifically, this paper will discuss methods and tools used to calculate and render air traffic densities over areas of interest, as well as methods for aggregating such traffic densities over different time scales to extract fluctuations and periodic cycles in traffic patterns. We apply these tools to study the effects of possible modifications to the current en-route aircraft separation requirements. These modification, which are based on the characteristics of large fixed wing aircraft, has the potential of increasing the amount of available air space, allowing for future increases in overall air traffic numbers. In addition, we apply the same suite of tools to provide a quick visual inspection of planned UAV operation under different aircraft separation requirements. The studies conducted in this paper are based on a data set provided by NASA's Aviation Systems Division in charge of air traffic management research. Our investigation shows that our tools can be used to aid evaluation processes to determine, and increase, potentially underutilized airspace.

## 2. Previous Work

The main thrust of this paper is on visual analysis of air traffic data. Hence, this section focuses on work related to visualizing air traffic data. One of the most popular technique for visualizing air traffic data is to represent the trajectory of each aircraft as an animated particle. Many such visualizations are available on the web via sites such as youtube. A version that was designed by Aaron Koblin [9], and accessible through <http://www.youtube.com/watch?v=H2qTwvaQ.F4>, demonstrates several techniques and embellishments for presenting the flight trajectories. More recently, the discrete nature of the flight tracks were smoothed out to obtain a continuous estimate of air traffic density using a view dependent kernel density estimator [10]. Representing air traffic data as a density plot is not new. Kellner [8] also used density plots of the arrival and departure rates of aircraft at different airports to assess their capacity. This paper will use similar techniques in visualizing the air traffic data. More importantly, our work examines the impact of varying minimum aircraft separation policy on air traffic density, and also examines if a flight plan, e.g. of a UAV operation request, will endanger existing flight patterns.

There are many factors affecting air traffic congestion and airport capacity. One of those that is controllable and fall under policy decisions is the specification

of minimum separation between aircraft. Currently, this is set to 5 nautical miles horizontally, and 1,000 feet vertically [4] when the aircraft is en-route. This limit is adjusted as the aircraft approaches an airport and can drop to 3 miles horizontally on landing approaches to airports. The relative weight class of the leading and following aircraft are also taken into consideration in such situations in order to reduce risks due to wake turbulence [3]. The en-route limit accounts for aircraft speed (typical passenger jets fly at average speed of 500 miles per hour or just over 8 miles per minutes), weather impact on visibility, and wake turbulence from leading aircraft, among other factors. With the touted capabilities of ADS-B, the NextGen enabled weather system, and integrated information system, one can theoretically safely reduce the minimum separation requirements between aircraft. This paper provides visual analysis tools to examine the effects of different shapes and parameters describing the minimum separation volume between aircraft.

With regards to UAV operation, they are more generally referred to as Unmanned Aircraft Systems (UAS) [7, 2]. Over the past few years, interest in UAS has rapidly increased. This is because of the possibilities they offer to both government and commercial interests. They would enable a broad range of satellite-like abilities, but at a much lower cost. Aerial photography, communications, environmental monitoring, and security are some of the abilities that UAS deployment could make possible on a large scale. Currently, UAS are predominantly used by the Department of Defense and the Department of Homeland Security, and often outside of national air space (NAS). A handful of UAS are allowed to operate inside our NAS, though almost exclusively for national security or research purposes. However, each UAS operation must be pre-approved by the FAA on a case by case basis. This process is very tedious and does not scale well to large numbers of flights. There are a few studies on risk management of operating UAS. A recent study uses a site-specific non-uniform probabilistic background air traffic to study the risks [11]. Using the visual analysis tools presented in this paper, checking whether the flight plan for a UAS will allow for a safe operation within the NAS can be accomplished expeditiously.

## 3. Air Traffic Density Volumes

Air traffic data usually consists of a collection of flight trajectories of different aircraft. Each flight trajectory usually contains information about the type of aircraft, origin and destination airports, followed by a series of entries that records the time, location, and

altitude of the aircraft. The flight tracks are usually recorded in 10 second intervals. Other information such as date, heading, velocity, etc. are generally recorded as well, but were not available in the data set used in our study. The data set used to test and demonstrate our visual analysis tool has an area of interest that is located in the north eastern part of North Dakota, specifically the greater Devils Lake and Grand Forks areas. It includes all flight path information from flights that took place over an area of approximately 190 by 165 miles, between the altitudes of 0 and 60,000 feet from the beginning of July 2008 to the end of June 2009. There are 349,992 unique flight path records in this particular data set. This data set is comprised of uniquely identified flight paths, each containing latitude, longitude, and altitude information at 10 second intervals for the duration of the flight within the area of interest. The time of day and month in which the flights took place are specified. However, the specific date the flight took place is not included.

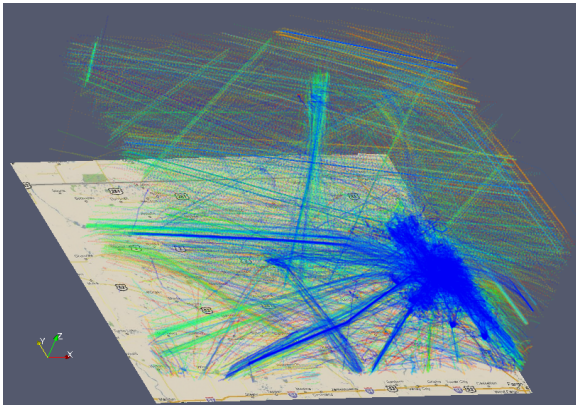


**Figure 1. Close to 350,000 flight tracks during the span of 1 year are overlaid into a single image. The tracks are colored depending on which month the flight occurred. Blue is for the last month in the data set. Individual tracks are rendered with 90% transparency so that some structure can be discerned from the data e.g. takeoff and landing patterns from regional airports. There is a vertical exaggeration of 10. The data set covers an area of approximately 190 miles by 165 miles in the north eastern portion of North Dakota. This figure represents altitudes between 0 and 60,000 feet. The large high density region on the right is over both the Grand Forks International Airport and Grand Forks AFB.**

An intuitive way to visualize flight paths is by representing each aircraft as a particle and animating the trajectory of each aircraft. This results in animations such as those found in [9]. An alternative way using only a single static visualization is to trace and overlay individual flight trajectories. Figure 1 shows an example of such a visualization. Note that because there are so many flight trajectories in this data set, displaying each path at full intensity will produce an extremely cluttered display. Instead, each path is rendered at only 10% opacity (90% transparency). It is only then that clusters of similar flight paths can be observed. These clusters can in turn be associated with local and regional airports and show the prevailing takeoff and landing patterns.

In this paper, we are interested in analyzing air traffic congestion as a result of policy changes to the separation minima criterion, as well as potential conflicts of UAS operations within the NAS. The flight trajectory data set in its current form is not directly suitable for such analysis. Instead, we need to create a conflict probability volume that characterizes the probability that an aircraft can be found in any location in space (and time) and would therefore be in conflict with another aircraft (or UAS). In order to create such a volume, we essentially need to convert the discrete flight tracks into a continuous volumetric data. The first issue in creating such a volume is to determine an appropriate discretization of the volume of space of interest. Another issue is how the discrete flight tracks are used to produce a smooth continuous volume.

There were two main factors that we considered in order to determine the spatial discretization. The first factor is the FAA's minimum aircraft separation criterion. This is referred to as the conflict boundary or more generally the separation minima. For en-route flights, this is specified to be 5 nautical miles horizontally (30,380 feet), and 1,000 feet vertically for each aircraft. Within the terminal area, this is lowered to 3 nautical miles. This criterion would have discretized our volume of interest (190 mi x 165 mi x 60,000 feet) into a 38 x 32 x 60 grid. That is, each aircraft takes up one voxel. The second factor is determining a good resolution to represent the approximate distance traveled by an aircraft in 10 seconds, the time resolution of the data. Given the presence of both commercial aircraft and many relatively slower general aviation and training aircraft used by the University of North Dakota Aerospace aviation school, there is no single all purpose resolution. Speeds can vary between 200 mph (2,900 feet per 10 seconds) for the slower personal and training aircraft, to 600 mph (8,800 feet per 10 seconds) for the faster passenger airliners. The vertical separa-

tion criterion is also greatly influenced by the relative weight class of the leading and following aircraft. Taking these factors into consideration, we decided to have each voxel represent a much smaller volume of 5,000 feet by 5,000 feet by 500 feet of airspace. Our volume of interest is thus discretized using a  $208 \times 174 \times 121$  grid. It should be noted that the volume of interest covers a much larger lateral area compared to its vertical extent. Thus in all our visualizations, there is a vertical exaggeration by a factor of ten. This exaggeration allows for easily discernible variations in altitude when viewing the volume from various angles.

The next step in calculating the conflict probability volume is to efficiently record the flight path information onto the grid. This process is discussed in the next section. Here, we discuss an alternative that also provides information about air traffic density. Basically, we want to create a density volume that records the number of aircraft found at each grid point over the duration of interest (e.g. every 10 second interval, hourly, monthly, or over the entire year). For this purpose, there are a number of options ranging from a simple nearest-grid-point (NGP) interpolation, where the location of an aircraft at each 10 second interval is associated with the grid point closest to it, to more sophisticated kernel based techniques. In this paper, we use the cloud-in-cell (CIC) interpolation [6]. Similar to NGP, the CIC method first determines the voxel that contains the flight data point. However, unlike NGP, CIC distributes the contribution of the flight data point amongst the 8 grid points of the voxel (instead of the single closest grid point). The contributions are weighted according to proximity of the data point to each grid point. The weighting function contains the product of three terms, each of which are linear in a dimension, with the total weighting normalized to unity. If a data point is respectively 25%, 40%, and 70% of the way across the cell from the lower front left corner in the three dimensions, we attribute  $0.75 \times 0.6 \times 0.3$  of the particle's mass to that corner [5]. This produces a smoother density volume, that does not incur the cost of more expensive methods such as kernel density estimates [13].

Once processed, the air traffic density volume (and later on, the conflict probability volume) needs to be visualized. To do this, we used ParaView [1] and the open source visualization toolkit Vtk [12] to help with our analysis. Two main visualization techniques were used. The first is direct volume rendering (for example, see Figure 2). While this technique does make relative high and low traffic areas discernible, it has a disadvantage. The internal 3D structures of the volume, particularly at busy regions such as near airports, are



**Figure 2. Direct volume rendering of the same data set that has been converted into a  $208 \times 174 \times 121$  grid using cloud-in-cell smoothing. The volume represents the average aircraft density over the course of a day at each location based on an entire year's worth of data. Opacity is mapped to density so more opaque bluish regions represent places with higher aircraft density. A nonlinear opacity map in order to see the air traffic corridors. A top down view of the region of interest is used in this figure.**

very difficult to discern without the aid of additional tools such as cutting planes. This can be alleviated to some extent by adjusting the transfer function used in the rendering. However, because the distribution of air traffic density is very skewed (towards very low aircraft counts, unless right over the airport), histogram equalization is needed to distinguish slight variations in aircraft densities. An alternative is to use isosurfaces. We specify different threshold values corresponding to different density of interest. The different isosurfaces corresponding to these different thresholds are then rendered as surfaces with different colors and opacity (see Figure 3).

As can be seen in Figure 2 the main thoroughfares are clearly visible as blue lines across the map. Areas with denser air traffic are also visible as blue shaded areas. However, it is hard to see distinct variations between low and high traffic areas other than as subtle variation of opacity in the shades of blue. This issue can be effectively handled with the application of isosurfaces. Once isosurfaces are applied, the resulting renderings are much more informative. Figure 3 shows

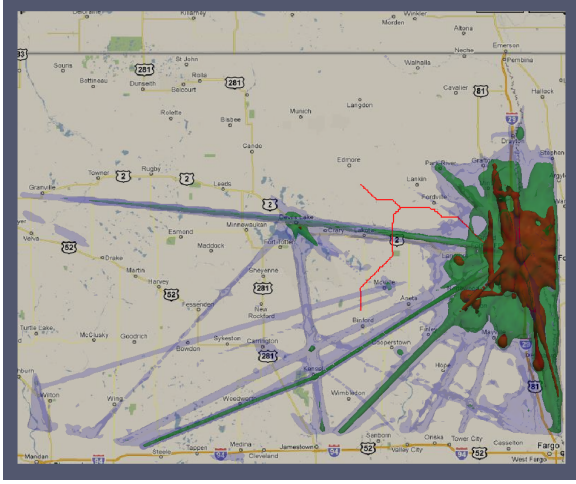


**Figure 3. Similar to Figure 2 but this time only the flight tracks between 0 and 15,000 feet elevation are depicted. Isosurface rendering is used instead of direct volume rendering. The isosurfaces colored blue, green, and red, represent densities of 25, 125, and 625 aircraft per voxel, respectively. Also visible are two proposed UAS tracks, shown in red. Both UAS tracks are below 10,000 feet.**

a rendering with three distinct isosurfaces. High and low traffic areas have become easily discernible, while still showing the main thoroughfares.

#### 4. Modifying the Separation Minima

The aircraft density volume described in the previous section and depicted in Figures 2 and 3 provides a sense of the air traffic over the region of interest. While the grid discretization took into account FAA’s separation minima, it was primarily driven by average aircraft speeds. In this section, we describe an alternate formulation that explicitly factors in the separation minima. This formulation is based on the conflict probability volume describe by Lee and Meyn [11], but modified to account for different conflict boundary shapes.

We first describe the conflict probability volume used in [11]. The separation criteria of 5 nm horizontal separation and 1,000 feet vertical separation essentially describes a conflict boundary that is the shape of a circular cylinder. Conflict probability refers to the probability that another aircraft can be found within this circular cylinder. Uncertainty arises from the sensors used in determining aircraft positions. Horizontal uncertainty is considered to be independent of

the vertical uncertainty since the horizontal coordinates come from radar data, while the vertical altitudes come from transponder data. The radar data came from the Advanced Synthetic Aperture Radar with a conservation uncertainty estimate of 0.125 nm, while the transponder altitude uncertainty is at most 100 feet. The contribution of each aircraft  $i$  to the conflict probability at position  $(x, y, z)$  is modeled as  $p_i(x, y, z) = p_{h_i}(x, y)p_{v_i}(z)$ . Where the horizontal probability  $p_{h_i}$  is modeled as a 2D Gaussian with standard deviation  $\sigma_h$ , and the vertical probability  $p_{v_i}$  is modeled as a 1D Gaussian with standard deviation  $\sigma_v$ .

$$p_{h_i} = \frac{1}{2\pi\sigma_h^2} \exp\left(-\frac{(x-x_i)^2 + (y-y_i)^2}{2\sigma_h^2}\right) \quad (1)$$

$$p_{v_i} = \frac{1}{\sqrt{2\pi}\sigma_v} \exp\left(-\frac{(z-z_i)^2}{2\sigma_v^2}\right) \quad (2)$$

The total conflict probability at a point is simply the sum of the contributions from each aircraft for the relevant time frame. To calculate the conflict probability volume, we calculate the conflict probability for each grid point normalized by the number of days (365 in this case).

This volume has some similarities and differences when compared to the air traffic density volume obtained using CIC. They are similar in that both produce a smooth volume based on the air traffic data and provides information about local traffic density or probability. They are different in that CIC uses a linear dropoff function of contribution within the voxel that contains the aircraft, while the latter uses a Gaussian dropoff function spread out over several voxels, up to 5 nm from the aircraft position. Also, the CIC volume provides average number of aircraft, while the conflict probability volume provides a probability of finding another aircraft.

In this paper, we investigate how the conflict probability volume is changed when the separation minima specification is changed. In particular, we examine the case when the shape of the conflict boundary volume is changed from a circular cylinder to an elliptical cylinder. The motivation is that aircraft, particularly large passenger or commercial planes, tend to maintain their current heading when en-route and make much smaller changes to their bearing. Thus, we can keep the 5 nm separation along the plane’s heading, and align this with the major axis of an ellipse. The minor axis is then aligned orthogonal to major axis, and can have a smaller separation minimum. The plane is still conservatively assumed to be centered in the ellipse to account for potential danger due to wake turbulence.



Minor \ Conflict	0	0.005	0.01	0.05
5 nm	14%	4.36%	1.68%	0.34%
4 nm	12%	3.45%	1.33%	0.27%
3 nm	9%	2.51%	0.98%	0.19%
2.5 nm	8%	2.04%	0.81%	0.14%
2 nm	7%	1.58%	0.64%	0.09%
1 nm	3%	0.72%	0.29%	0.02%

**Table 1. Effects of changing the separation minimum along the minor axis (orthogonal to aircraft heading) on the percentage of conflict probability volume using different safety margins. For example, 1.33% of the volume has a conflict probability of .01 or less if the minimum separation along the minor axis is set to 4 nm.**

The vertical components remain unchanged. The formulation for the contribution of individual aircraft to the conflict probability volume is modified to be the product of 3 one dimensional Gaussian distributions. These represent the Gaussian distributions along the major axes, the minor axis, and the vertical axis of each aircraft. The uncertainty in the horizontal location  $p_{h_i}$  is separated into two one dimensional components:  $p_{M_i}$  and  $p_{m_i}$  to represent the uncertainty in positions along the major and minor axes respectively. The uncertainty in the vertical location is the same as the previous formulation for  $p_{v_i}$ .

We experimented with various values of separation minimum for the minor axis and studied their impact on the reduction of conflict probability (which is proportional to air traffic congestion) for different safety margins. Table 1 shows the effects of varying the minor axis from the original 5 nm down to 1 nm. The column headings indicate different thresholds on the conflict probability volume. Entries in the table indicate the percentage of grid points that are at or below the safety margin. Not surprisingly, as we reduce the separation minimum along the minor axis, we expect to see a reduction in the conflict probability. These effects are better seen in Figure 4 which shows the mostly linear relationship between separation minimum of the minor axis and the reduction in the conflict probability (expressed as a ratio of the conflict probability using a different minor axis against the conflict probability where the minor axis is 5 nm). These results are bolstered by the visualizations showing how the conflict probability volume appears for two different separation minimum of the minor axis, illustrated in Figure 5.

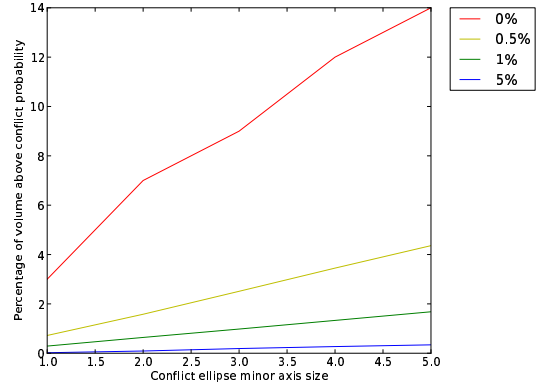


**Figure 4. The same information as in Table 1 showing the linear relationship between the reduction of the percentage of air space volume that is in conflict as the minor axis is reduced. The different curves are for different thresholds of the conflict probability. So, the blue curve shows the percentage of volume that is above the 5% conflict probability threshold as a function of minor axis separation distance.**

## 5. Analysis of UAS Tracks

The conflict probability volume constructed based on the separation minima can also be used in the analysis of UAS trajectories. UAS operations are granted approval based on their impact on their safe operation within the NAS. This can be achieved by minimizing the cumulative conflict probability along their paths, and ensuring that the conflict probabilities everywhere along their trajectories are below some threshold.

We obtained two UAS tracks originating from the Grand Forks Air Force Base (RDR). One track goes towards the Tiger military operation area (MOA) along the northern corridor while the other goes towards the Devils Lake MOA along the southern corridor. Both tracks share a common initial track from the RDR. They are theoretically optimal tracks with the least conflict route from RDR to the north and south MOAs. These tracks can be seen in Figures 3 and 6. Note that unlike the aircraft trajectory data, the UAS tracks were derived based on the resolution of the conflict probability grid. Hence, one can observe the jagged nature of their trajectories.

The two UAS paths do not go above 10,000 feet. To get a less cluttered visualization, we do not show air traffic above 15,000 feet. Once the initial trajectory

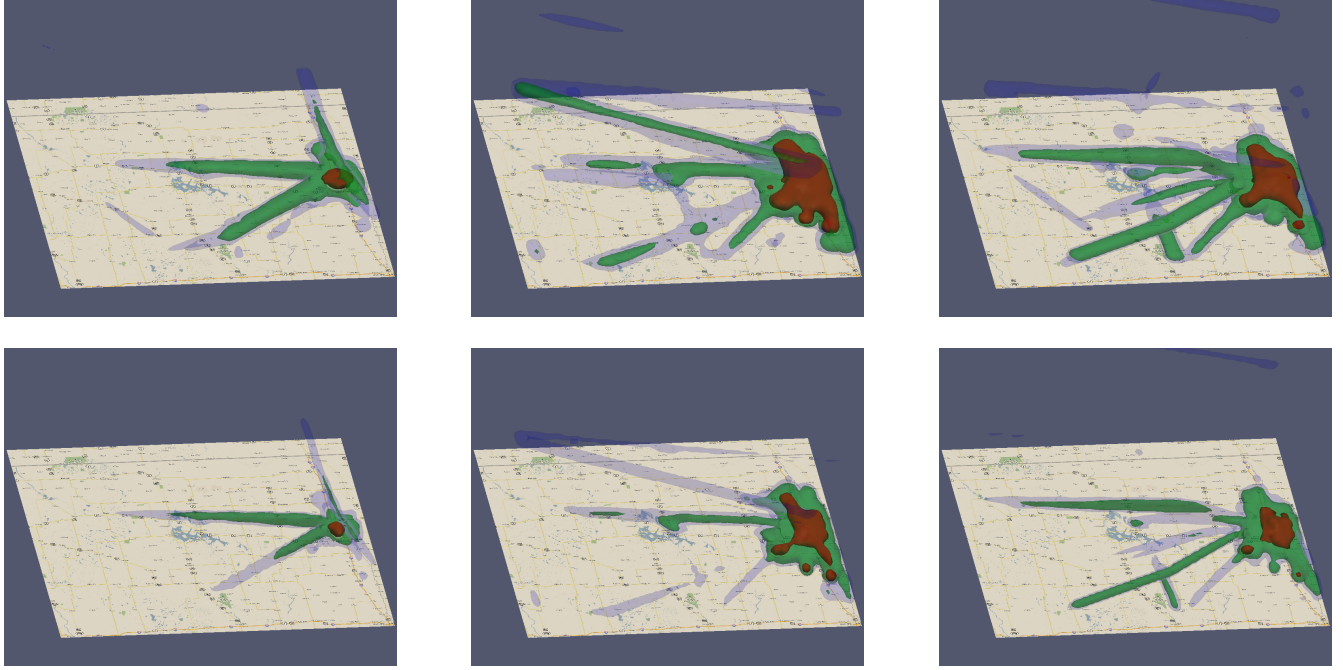


**Figure 5.** The first row shows the conflict probability volumes using 5 nm for the minor axis separation, while the second row uses 2.5 nm for the minor axis separation. The first column shows the conflict probability volumes for 6am CMT when we see the first surge of morning traffic. The next two columns show the conflict probability volumes for 9am and 6pm CMT respectively. These images show the spatial context for the reduction in conflict probabilities (and the air traffic density) as a result of reducing the separation minimum of the minor axis from 5nm to 2.5nm. Isosurface colors correspond to thresholds of .05% in blue, 1% in green and 5% in red. The quantitative changes in conflict volumes are shown in Table 1.

clears the local RDR terminal air space, we can observe that the north bound UAS path is relatively clear of any high air traffic areas. On the other hand, the south bound UAS path not only leads to an area surrounded by high air traffic, but this path even passes through a rather large thoroughfare, depicted by the green isosurface in Figure 6. After showing this potential problem with the southern track to the track developers, we were given two reasons: (i) The UAS headed to the Devil Lake MOA along the southern corridor initially headed north in order to reduce the amount of time spent in the high traffic region e.g. compared to if it headed directly towards the Devil Lake MOA. The amount of time in the high traffic region is directly proportional to the conflict probability of the track. (ii) The grid that was used to develop the tracks essentially had horizontal information only. The vertical component of conflict probability was modeled as a simple linearly decreasing function up till 6,000 feet. Using the visual analysis tools, one can quickly examine and see

potential conflicts of planned UAS trajectories against the prevailing air traffic patterns for a given area of operation.

Since Figure 6 is based on daily averages, we sought to answer the question whether there are particular times during the day when it is safer relative to others. Obviously, flying during non-peak hours e.g. before 6am or late at night would reduce potential conflicts. In fact, from midnight to 5am, and after 10pm, the southbound UAS track does not intersect with the green traffic region. However, these may not be the times required for the UAS operations. Between 6am and 9pm, we found that the southbound UAS track has significantly reduced conflict probability between 10am and 5pm CMT (see Figure 7). Note that while the southbound UAS penetrated the green zone (at or over 125 aircraft per day) in Figure 6, it is above the green zone (at or over 1% conflict probability) in Figure 7.

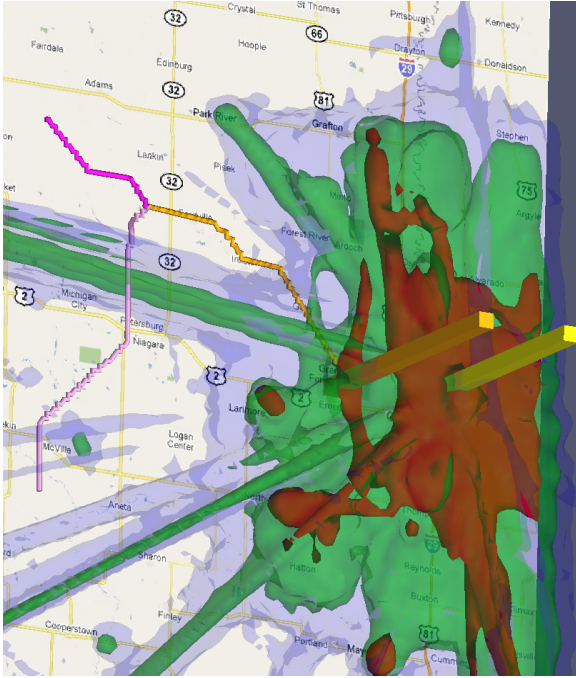


**Figure 6. Zoomed in view of Figure 3. The UAS tracks are now colored differently to indicate the overlapping segment as well as the norther and southern forks. The two tall rectangular volumes indicate the locations of the two airports. The origination airport of the two UAS tracks is the Grand Forks Air Force Base on the left. The UAS headed along the southern corridor clearly intersects the green isosurface, which represents at least 125 aircraft per day on average.**

## 6. Conclusions and Future Work

This paper presented visual analysis tools for studying air traffic data. We demonstrate the utility of the tools using two different applications. First, we study the impact of changing the separation minima for aircraft on the conflict probability volume. This is one of the first considerations if aircraft are to fly closer to each other using the NextGen infrastructure. Second, visual analysis of UAS request to quickly see the trajectory in relation to the air traffic density (and hence conflict probability) in its theater of operation.

The tools developed so far just provides a glimpse of what visual analysis has to offer. There are some obvious rooms for enhancements. The conflict probability volume is currently based on air traffic trajectories only, but do not take into account the weight class

of the aircraft, the flight phase of the aircraft, environmental constraints such as prevailing winds, mountain ranges, etc. Taking these other relevant factors into account can provide a more accurate conflict probability volume. Also, while the visual analysis of UAS requests allows one to quickly identify potential conflicts, it operates under the assumption of an advance request. Future enhancements can incorporate dynamic modifications to the UAS flight plan that would take into account varying weather conditions as well as unforeseen deviations from the normal traffic patterns on flight day. Visual analysis such as the one described in this paper are enabling tools that will help make the visions of NextGen a reality.

## References

- [1] *ParaView Guide*. Kitware, Version 3 (February 2008). <http://www.paraview.org>.
- [2] E. Atkins. Risk identification and management for safe UAS operation. In *Systems and Control in Aeronautics and Astronautics (ISSCAA)*, 2010. [http://ieeexplore.ieee.org/xpl/freeabs\\_all.jsp?arnumber=5632396](http://ieeexplore.ieee.org/xpl/freeabs_all.jsp?arnumber=5632396).
- [3] FAA. Pilot and air traffic controller guide to wake turbulence. [http://www.faa.gov/training\\_testing/training/media/wake/04SEC2.PDF](http://www.faa.gov/training_testing/training/media/wake/04SEC2.PDF).
- [4] FAA. Order JO 7110.65s air traffic control, 2008. <http://www.faa.gov/documentLibrary/media/Order/7110.65S.pdf>.
- [5] J. Faber, J. James C. Lombardi, and F. Rasio. StarCrash: A parallel smoothed particle hydrodynamics (SPH) code for calculating stellar interactions. <http://ciera.northwestern.edu/StarCrash/manual/usersmanual.pdf>.
- [6] R. W. Hockney and J. W. Eastwood. *Computer simulation using particles*. Taylor & Francis, Inc., Bristol, PA, USA, 1988.
- [7] L. D. Jr. and A. Duquette. Fact sheet – unmanned aircrafts systems (UAS). [http://www.faa.gov/news/fact\\_sheets/news\\_story.cfm?newsId=6287](http://www.faa.gov/news/fact_sheets/news_story.cfm?newsId=6287).
- [8] S. Kellner. Airport capacity benchmarking by density plots. In *Deutscher Luft- und Raumfahrtkongress (German Aerospace Congress)*, 2009.
- [9] A. Koblin. Flight patterns. <http://users.design.ucla.edu/~akoblin/work/faa>.
- [10] O. Lampe and H. Hauser. Interactive visualization of streaming data with Kernel Density Estimation. In *Pacific Visualization Symposium (PacificVis)*, 2011. [http://www.youtube.com/watch?v=1N5kg\\_tcG1s](http://www.youtube.com/watch?v=1N5kg_tcG1s).
- [11] H.-T. Lee and L. Meyn. Traffic impact study of unmanned aerial vehicle operations over the grand forks air force base area. Report submitted to the US Air Force, 2009.
- [12] W. Schroeder, K. Martin, and B. Lorensen. *The Visualization Toolkit: An Object-Oriented Approach to 3D Graphics*. Prentice Hall, New Jersey, 1996.
- [13] B. W. Silverman. *Density Estimation for Statistics and Data Analysis*. London: Chapman and Hall, 1986.



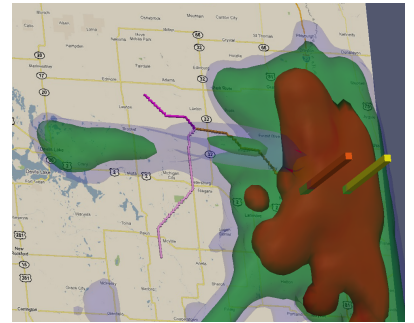
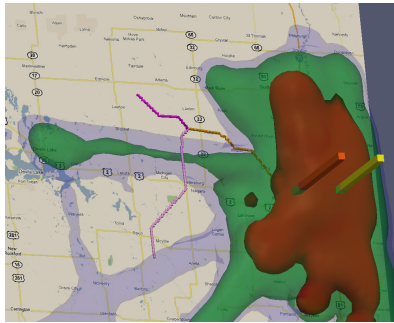
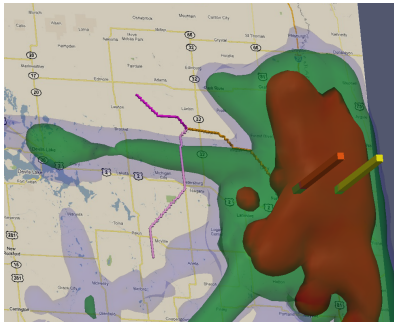


**Figure 7. Details on the southbound UAS track for 10am, 11am and 12 noon CMT. Isosurface colors correspond to thresholds of .05% in blue, 1% in green and 5% in red in conflict probabilities. Here, we can see that the southbound UAS track has conflict probability of less than 1% at these times.**